

Research Article

Assessment of *in vitro* Cytotoxic, iNOS, Antioxidant and Photodynamic Antimicrobial Activities of Water-soluble Sulfonated Phthalocyanines

Mustafa Akin¹, Neslihan Saki^{2*} , Emre Guzel³ , Batuhan Orman⁴, Ayse Nalbantsoy⁵ and Makbule B. Kocak⁶ 

¹Petroyağ and Kimyasallar San. Tic. A.Ş., Research and Development Center, Kocaeli, Turkey

²Department of Chemistry, Kocaeli University, Kocaeli, Turkey

³Department of Engineering Fundamental Sciences, Faculty of Technology, Sakarya University of Applied Sciences, Sakarya, Turkey

⁴Department of Biotechnology, Graduate School of Natural and Applied Sciences, Ege University, Izmir, Turkey

⁵Department of Bioengineering, Faculty of Engineering, Ege University, Izmir, Turkey

⁶Department of Chemistry, İstanbul Technical University, İstanbul, Turkey

Received 26 July 2021, accepted 1 November 2021, DOI: 10.1111/php.13558

ABSTRACT

In recent years, much effort has been devoted to the development of effective anticancer agents. In this manner, the utilization of water-soluble sulfonated phthalocyanines is crucial for many cancer cell lines. In this study, phthalonitrile and metallophthalocyanine compounds linked by benzenesulfonic acid groups have been prepared. Antimicrobial behaviors of those compounds were investigated by performing disk diffusion and photodynamic assays on gram-positive and negative bacteria. Indium phthalocyanine (InCIPc) (3) showed inhibition activity against *B. cereus*, *B. subtilis* and *S. aureus* with disk diffusion assay. Also, gallium and indium phthalocyanines (2 and 3) exhibited inhibitory activity on both gram-positive and -negative microorganisms after light activation. Increasing the inhibitor concentration and light exposure time increased the inhibition activity for both molecules. GaCIPc (2) demonstrated the maximum reducing power capacity among studied compounds, and CoPc (4) showed even better DPPH radical scavenging ability than the standard molecule Trolox at 2000 $\mu\text{g mL}^{-1}$ concentration. The dose-dependent effect of compounds on cytotoxicity was studied against cancer cells PANC-1, MDA-MB-231, HepG2, A549, HeLa, CaCo-2 and non-tumorigenic cells HEK-293. All compounds showed no significant cytotoxic effect on any cell line up to the highest treated concentration at 50 $\mu\text{g mL}^{-1}$. However, all phthalocyanines had significant nitric oxide inhibition activity, and only in copper phthalocyanine (CuPc) (5), the MTT IC_{50} value was reached on LPS-activated RAW 264.7 macrophage cells. The lowest inducible nitric oxide synthase (iNOS) IC_{50} values were defined as $6 \pm 1 \mu\text{g mL}^{-1}$ and $7 \pm 0.5 \mu\text{g mL}^{-1}$ for CuPc (5) and InCIPc (3), respectively.

INTRODUCTION

Phthalocyanines (Pcs) were found by chance at the beginning of the 20th century, and its structure was elucidated after 1928, as it became commercially important. It has been used as a dye and pigment for many years. In recent years, it has been investigated in technological applications such as liquid crystal (1), photovoltaic (2), catalysis (3), chemical sensors (4,5) and photodynamic therapy of cancer (PDT) (6–9). Pcs are among the most preferred materials in PDT applications (10). The most important reasons for this are its strong absorption at the phototherapeutic window where tissue penetration line is maximized, low dark toxicity and aqueous solubility properties (11–13). These compounds have no solubility in almost all solvents, when not substituted, due to the intense π -conjugated aromatic nature. However, to overcome this problem, generally, the two important parameters for synthesizing soluble phthalocyanines are appropriate; metal and substituent selection (14). The substitution of a diversity of peripheral or axial groups, metal insertion, variation of the macrocycle's main structure and extension of conjugation has a strong influence on the solubility and electronic absorption characteristics (15,16). Especially, the metal atom in the center of phthalocyanines significantly affects both the solubility of the complex and its photophysical and photochemical properties (17–19). In topical, interstitial and direct injection into the blood system PDT applications, since blood is a hydrophilic system, water solubility is crucial for a potential photosensitizer in PDT. It has been reported that by using appropriate hydrophilic substituents in phthalocyanines, both water solubility is achieved and their aggregation tendency is reduced (20–23). Anionic/hydrophilic substituents usually used to ensure water solubility to phthalocyanines are carboxylate, sulfonate and phosphorus-based functional functionalities that can be linked directly with the macrocyclic ring or various spacers (14,24). Most of the anionic phthalocyanines synthesized for PDT contain sulfonate or sulfonic acid groups (25).

Antibiotic resistance, an increasingly common problem in pathogens, has encouraged the search for new antimicrobial

*Corresponding author email: sakineslihan1@gmail.com (Neslihan Şaki)
© 2021 American Society for Photobiology

routes in recent times and treatment of local infections with photodynamic antimicrobial therapy brought a new perspective in pharmacy. By using this therapy, the microorganisms are exterminated by the action of photosensitizers and suitable light. While photosensitizers do not have antimicrobial effects alone, reactive cytotoxic products formed as a result of irradiation with light in the presence of oxygen damage microbial cells (26,27). Two mechanisms explain the fatal damage inflicted by bacteria. When DNA damage occurs, leakage of cellular contents and cytoplasmic membrane damage are caused by the inactivation of enzymes involved in membrane transport systems (28). This method is mostly used in the treatment of local infections that turn out to be chronic after long-term antibiotic treatments. On the contrary to antibiotics, reactive oxygen species formed during photodynamic antimicrobial inactivation interact with structures of cells and different metabolic routes in microbial cells, so repeated photosensitization of bacteria does not induce the selection of resistant strains. This treatment can be applied if it is tolerated by the patient to be treated for local infection (29).

Oxidative stress displays a role in the emergence of numerous chronic diseases like cardiovascular disease, diabetes, cancer and some neurological diseases. Oxidative stress related to free radicals in biomolecular reactions has been reported in many scientific studies (30). The antioxidant potentials of Pcs have been the subject of many studies, and their distinctive chemical and physical properties coming from π systems are delocalized over an arrangement of conjugated carbon and nitrogen atoms.

Inflammation is an important and complex defense mechanism and can be involved in the regulation of various inflammatory diseases and physiological functions; however, in chronic cases, it causes undesirable side effects (31). Inhibition of NO (nitric oxide) generation via LPS-induced in RAW 264.7 cells can provide information about the anti-inflammatory character of the compounds. Although there are not many studies on the effects of these compounds on the immune system, it has been reported in previous studies that phthalocyanines may have immunoregulatory effects (32). Also, new alternative anticancer methods should be investigated due to the deficiencies of known treatment methods of cancer. The anticancer effects of Pcs and their conjugates have been demonstrated by photodynamic therapy (33,34). Therefore, they are potential anticancer agents and further investigation should be conducted.

Herein, possible antioxidant and antimicrobial activities of six tetrasubstituted sulfonated metallophthalocyanines were evaluated. In the literature, there are few studies in which sulfonated phthalocyanines are used with iNOS, antimicrobial photodynamic and *in vitro* cytotoxic activity properties (35–38). However, this is the first study of anionic phthalocyanines containing benzene-sulfonic acid groups. The disk diffusion assay was performed to investigate the antimicrobial behaviors of the Pcs, and the photodynamic antibacterial inhibition properties of the compounds in different concentrations were tested against *S. aureus* and *E. coli*. Antioxidant properties of the Pcs were examined by carrying out the free radical scavenging and reducing power assays. Dark cytotoxicity of the compounds was performed by MTT test against several cancer cell lines which are PANC-1, MDA-MB-231, HepG2, A549, HeLa, Caco-2 and a non-tumorigenic cell line HEK-293. In addition, the effects of the compounds on the inducible nitric oxide synthase (iNOS) enzyme and their anti-inflammatory potential were explored on LPS-induced RAW 264.7 cells.

MATERIALS AND METHODS

General synthesis procedures for phthalocyanines. Our group prepared 4-(2,3-dicyanophenoxy)benzenesulfonic acid (1) and its gallium, indium and cobalt phthalocyanine derivatives (2–4) according to the reported procedure (39,40). For preparing the other phthalocyanines (5–7), in the complexation step, a mixture of 4-(2,3-dicyanophenoxy)benzenesulfonic acid (0.100 g, 0.32 mmol), anhydrous metal salts (CuCl_2 , MnCl_2 and NiCl_2 , ~0.11 mmol) and DBU (0.5 mmol) in *n*-pentanol (1.5 mL) was refluxed for 24 h. The reaction mixture was precipitated by the addition of *n*-hexane. The crude product was washed several times with ethanol, methanol and ethyl acetate to remove the impurities. The salt-formed product was dissolved in HCl solution (60 mL, 0.9 M), then precipitated with acetone, dried *in vacuo* at 100°C.

Copper (II) phthalocyanine (5). Yield: 0.029 g, 28%, FT-IR ($\nu_{\text{max}}/\text{cm}^{-1}$): 3070, 3030 (w, C-H), 1582 (m, Ar), 1224 (s, R-O-Ar), 1178 (m, S = O asym.st), 1122 (s, SO_3H), 1030 (s, S = O sym. st.). UV-Vis λ_{max} (nm) DMSO: 695, 625, 334. MALDI-TOF-MS m/z : 1304.70 $[\text{M} + \text{K} + \text{H}]^+$. Anal. calcd. for $\text{C}_{56}\text{H}_{32}\text{N}_8\text{O}_{16}\text{S}_4\text{Cu}$: C, 53.18; H, 2.55; N, 8.86, found: C, 53.02; H, 2.48; N, 8.96.

Manganese (II) phthalocyanine (6). Yield: 0.035 g, 34%, FT-IR ($\nu_{\text{max}}/\text{cm}^{-1}$): 3066, 3036 (w, C-H), 1582 (m, Ar), 1218 (s, R-O-Ar), 1175 (m, S = O asym.st), 1121 (s, SO_3H), 1032 (s, S = O sym. st.). UV-Vis λ_{max} (nm) DMSO: 755, 677, 516, 331. MALDI-TOF-MS m/z : 1297.25 $[\text{M} + \text{K} + 2\text{H}]^+$. Anal. calcd. for $\text{C}_{56}\text{H}_{32}\text{N}_8\text{O}_{16}\text{S}_4\text{Mn}$: C, 53.55; H, 2.57; N, 8.92, found: C, 53.42; H, 2.48; N, 8.98.

Nickel (II) phthalocyanine (7). Yield: 0.035 g, 34%, FT-IR ($\nu_{\text{max}}/\text{cm}^{-1}$): 3090 (w, C-H), 1582 (m, Ar), 1218 (s, R-O-Ar), 1172 (m, S = O asym.st), 1122 (s, SO_3H), 1029 (s, S = O sym. st.). UV-Vis λ_{max} (nm) DMSO: 691, 620, 328. $^1\text{H-NMR}$ (300 MHz, DMSO-d_6): δ , ppm 8.02–7.62 (4H, Pc-Ar-H) 7.60–7.22 (16H, m, Ar-H and Pc-Ar-H), 7.18–7.00 (8H, m, Ar-H). MALDI-TOF-MS m/z : 1339.40 $[\text{M} + 2\text{K} + 2\text{H}]^+$. Anal. calcd. for $\text{C}_{56}\text{H}_{32}\text{N}_8\text{O}_{16}\text{S}_4\text{Ni}$: C, 53.39; H, 2.56; N, 8.89; found: C, 53.22; H, 2.48; N, 8.92.

Antimicrobial activity. Disk diffusion method. Antimicrobial activities of the synthesized Pcs were explored for *E. coli* (ATCC 25922), *B. cereus* (ATCC 14579), *B. subtilis* (ATCC 6051) and *S. aureus* (ATCC 25923) by using the disk diffusion method. Mueller-Hinton Broth (MHB) was used for the incubation of bacterial cultures. Overnight incubated microorganisms were taken into the sterile tubes having 5 mL sterile pure water then adjusted to the 0.5 McFarland standard (1.5×10^8 CFU mL^{-1} of bacteria) spectrophotometrically. Cultures from these sterile tubes were inoculated to the petri dishes comprising Mueller-Hinton Agar (MHA), and Pcs were dissolved in water at 1 mg mL^{-1} concentrations. The disks were impregnated with 20 μL of prepared solutions and placed on the inoculated agar. Ampicillin (10 μg disk $^{-1}$) and cefotaxime (30 μg disk $^{-1}$) were chosen as positive reference standards. Lastly, inoculated petri dishes were incubated at 37°C for 24 h at the incubator, and antimicrobial properties were elucidated by evaluating the inhibition zone for the studied microorganisms (41).

Photodynamic antibacterial therapy. Bacterial cultures were cultivated in MHB at 37°C for overnight. An aliquot of these cultures (100 μL) was aseptically transferred to fresh MHB and grown at 37°C to have the 0.5 McFarland standard spectrophotometrically. After 2 h incubation at 37°C, Pcs at final concentrations of 0.25, 0.5 and 1 mg mL^{-1} were transferred into the tubes containing microorganisms and tested against microorganisms by irradiating with low-laser light (20 J cm^{-2} and 670 nm) for 60 and 12 min. The turbidimetric method was served to measure the optical density at 600 nm, and control tests were performed without the illumination of the cells with Pc compounds. Photoinactivation efficiency was revealed by measuring the turbidity of the tested and control samples spectrophotometrically (42).

Antioxidant activity. DPPH radical scavenging activity. DPPH (2,2-Diphenyl 1-picrylhydrazyl) free radical scavenging capacities of the Pcs were investigated (43). Different concentrations of Pcs in water and Trolox as the positive control were used as test solutions. 1 mL of Pc solution was mixed with 1mM DPPH solution, incubated for 1 h at dark, and the absorbance was measured at 517 nm spectrophotometrically. The control sample was prepared without the Pc compound. The DPPH radical scavenging activity percentage was calculated by using the following formula:

$$\text{DPPH scavenging activity (\%)} = \frac{A_{\text{sample}} - A_{\text{control}}}{A_{\text{control}}} \times 100$$

where A control and A sample indicate the absorbance of the control reaction mixture and sample, respectively.

Reducing power. Reducing power activities of Pc molecules was evaluated based on the method described previously (44). The mixture of sodium phosphate buffer with a pH of 6.6 (2.5 mL, 200 mM) and 2.5 mL potassium ferricyanide (1%) with 1 mL of sample was incubated at 50°C for 20 min. After the addition of 2.5 mL of 10% trichloroacetic acid, the mixture was centrifuged at RCF= 1100 g for 10 min. Then, 2.5 mL of the upper layer was taken in a tube, and 2.5 mL of deionized water and 0.5 mL of 0.1% ferric chloride were added. At last, the absorbance was read at 700 nm performing UV-Vis spectrophotometer. BHA was chosen as the control.

Cytotoxicity assay. Cytotoxicity was evaluated by the 3-(4,5-dimethyl-2-thiazolyl)-2,5-diphenyl-2H-tetrazolium bromide (MTT) colorimetric assay. Cancer cell lines, PANC-1 (human pancreatic carcinoma cells), MDA-MB-231 (human breast adenocarcinoma cells), HepG2 (human hepatocarcinoma), A549 (lung carcinoma cells), HeLa (cervix adenocarcinoma cells) Caco-2 (human colon carcinoma) cells and non-tumorigenic 293 HEK (human embryonic kidney cell line) cells were cultured in Dulbecco's modified Eagle's F12 medium (DMEM/F12) supplemented with 10% fetal bovine serum which was used to determine cytotoxicity based on previous study (45).

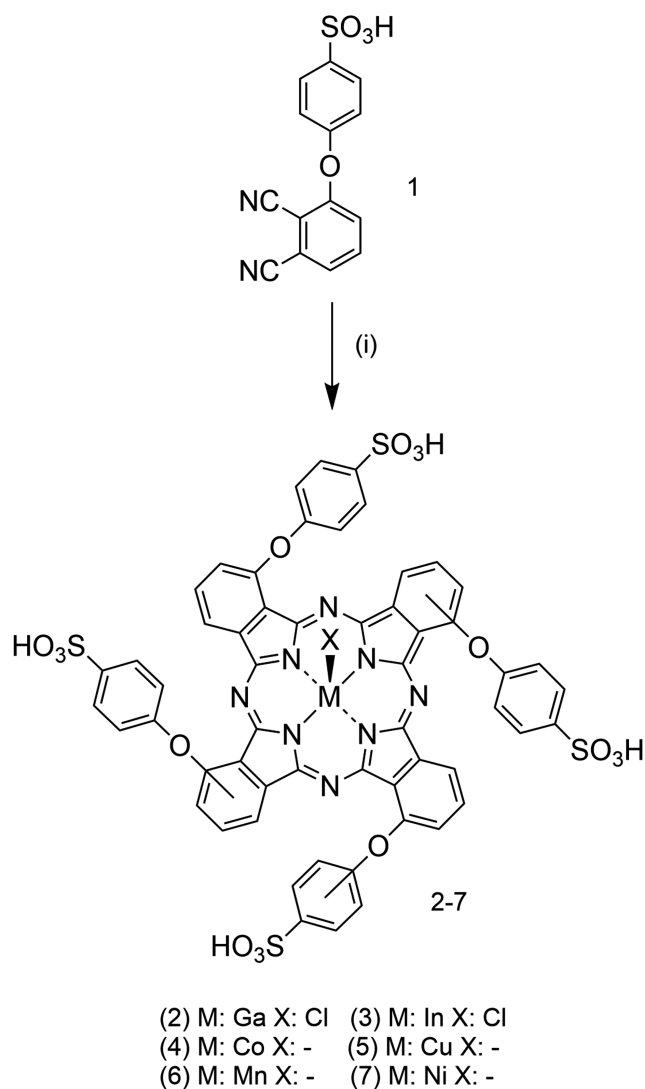
Inhibition of iNOS activity. The total amount of nitrite in a medium was used as an indicator of nitric oxide synthesis (46), and the inhibition of iNOS activity was determined in LPS-induced mouse macrophages (RAW264.7) as previously described (41). Cells were cultured in Roswell Park Memorial Institute (RPMI) 1640 medium supplemented with 10% heat-inactivated FBS, 2 mM L-glutamine and %0.1 penicillin/streptomycin (Gibco). Doxorubicin was chosen as the positive control. The compounds were also tested using MTT analyses to determine the cytotoxic activity for RAW264.7 cells.

RESULTS AND DISCUSSION

Synthesis and characterization

We aimed the synthesis of anionic water-soluble metallophthalocyanines using 4-(2,3-dicyanophenoxy)benzenesulfonic acid (**1**) for the determination of antimicrobial and anticancer potentials. Scheme 1 displays the synthetic pathway for water-soluble phthalocyanines (**2-7**).

Water-soluble phthalocyanines were obtained by cyclotrimerization of **1** using metal chloride salts as the template in the presence of DBU as the base and 1-pentanol as the solvent. To isolate these phthalocyanines (**2-7**), firstly they were treated with ethyl acetate, ethanol and cold methanol to remove the decomposition products and unreacted starting materials. After the products were treated with HCl solution and reprecipitated with an excess of acetone, they finally dried *in vacuo* at 100°C. Substitution of benzenesulfonic acid groups to phthalocyanine skeleton brings hydrophilic character to compounds and provides water solubility property. The novel compounds were elucidated by general spectroscopic methods. The spectroscopic data are consistent with the proposed structures. FT-IR spectra of the phthalocyanine compounds (**2-7**) showed aromatic (–CH) stretching peaks at 3066–3030 cm⁻¹, sulfoxide groups (–S = O) at 1033–1018 cm⁻¹ and sulfone groups (–O = S=O) at 1186–1180 cm⁻¹ (Figures S5, S6 and S7). The ¹H-NMR spectrum of phthalocyanine **7** showed the expected chemical shifts for the phthalocyanine structure. Detected aromatic protons were observed as multiplets between 9.22 and 7.22 ppm and 7.12–7.00 ppm for phthalocyanine **7**. Due to the paramagnetic character of copper, and manganese, there is no signal for compounds **5** and **6** in ¹H-NMR spectroscopy. MALDI-TOF mass results



Scheme 1. Synthetic pathway of the phthalocyanines (i) metal salts, n-pentanol, DBU, reflux, 24h.

confirm our proposed structures with molecular ion peaks at $m/z = 1304.70 [M + K+H]^+$, 1297.25 $[M + K+2H]^+$ and 1339.40 $[M+2K+2H]^+$ for **5**, **6** and **7**, respectively (Figures S2, S3 and S4).

UV-Vis absorption studies

The first and simplest method showing the formation of phthalocyanines is the absorption spectroscopy technique. Phthalocyanine complexes show characteristic electronic spectra in two absorption regions. One of them is in the UV region at 300–350 nm (B band), and the other one in the visible area at 600–700 nm (Q-band). The absorption spectra of the phthalocyanines were obtained in DMSO. The spectra of the phthalocyanines exhibited in the Q band region at 711 nm for **2**, 710 nm for **3**, 690 nm for **4**, 695 nm for **5**, 755 nm for **6** and 691 nm for **7** (Fig. 1). Besides, for manganese phthalocyanine (**6**), the band at 515 nm is attributed to the charge transfer between the Pc ligand and the central Mn ion.

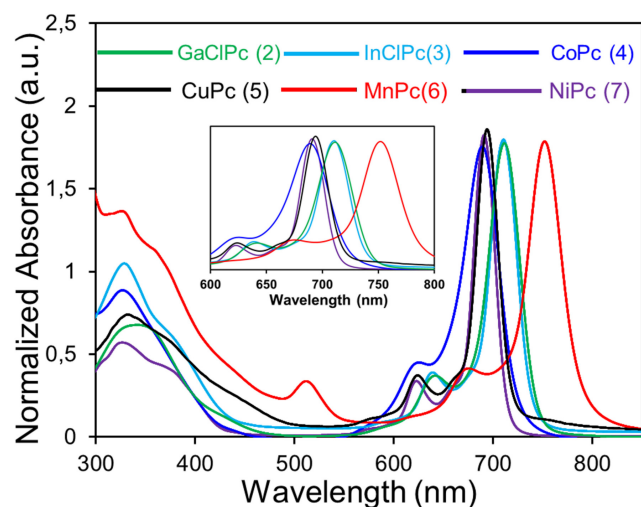


Figure 1. UV-Vis absorption spectra of phthalocyanines (2–7) in DMSO.

Aggregation of phthalocyanines can occur due to aromatic π -interactions and/or interactions between metal–ligand (LM) and substituents or solvent molecules. This aggregation is often shown as a coplanar combination of rings with the generation of dimer and higher-order structures from the monomer and is driven by the van der Waals attractive forces between the phthalocyanine rings. In the aggregated situation, the electronic structure of the phthalocyanine rings is perturbed, which can cause changes in the ground state and excited state properties. Thereby, the aggregation behavior of phthalocyanines may limit the photo-physical, photochemical and anticancer properties (47). This behavior of phthalocyanines can be changed by many factors such as concentration, temperature, the chemical composition of the medium and the solvent (40) (Figure S8). In this manner, the aggregation behavior of the copper phthalocyanine (5) was examined in different solvents (DMSO and water). The absorption spectrum of copper phthalocyanine (5) in water contains a broad Q band centered at 695 nm in a manner that is typical of aggregated phthalocyanines in a cofacial arrangement. When dimethyl sulfoxide (DMSO) was used, no aggregation formation is observed, because Q bands are sharp intense in DMSO whereas sharply decrease in water (Fig. 2). Also, the density of the Q-band in water is much lower than in DMSO, indicating intermolecular aggregation of copper phthalocyanine (5).

Antimicrobial activity

Disk diffusion method. The antimicrobial properties of Pcs were assessed by using the disk diffusion assay. Each disk was impregnated with 20 μ L Pc solution at 1 mg/mL concentration. According to the results, only InClPc (3) showed antimicrobial activity against gram-positive bacteria. When the obtained inhibition areas are examined, compound 3 created moderate inhibition zones compared with the standard antibiotics forming 8 mm against *B. subtilis* and *S. aureus*, 11 mm for *B. cereus* (Table 1). In this study, the effect of differences in the central metal atom on Pc compounds with the same substituents was investigated. It is known that the central metal atom and the attached substituent groups are effective in antimicrobial activity studies of Pcs (48,49). The inhibition mechanism of microorganisms can be

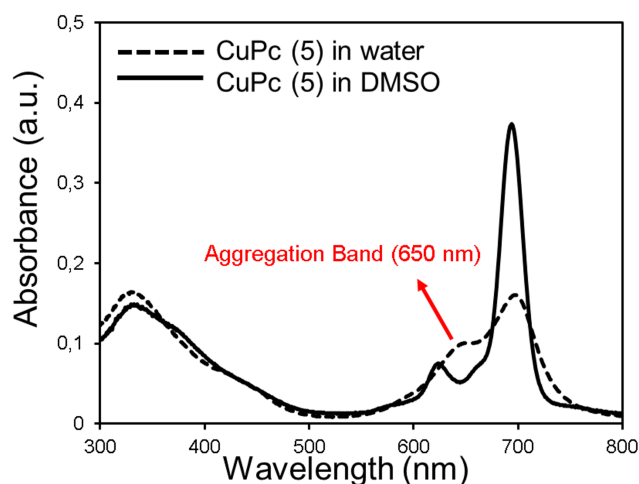


Figure 2. UV-Vis absorption spectra of copper phthalocyanine (5) in DMSO and water.

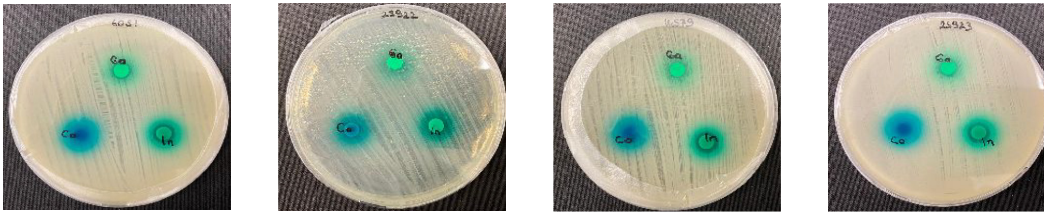
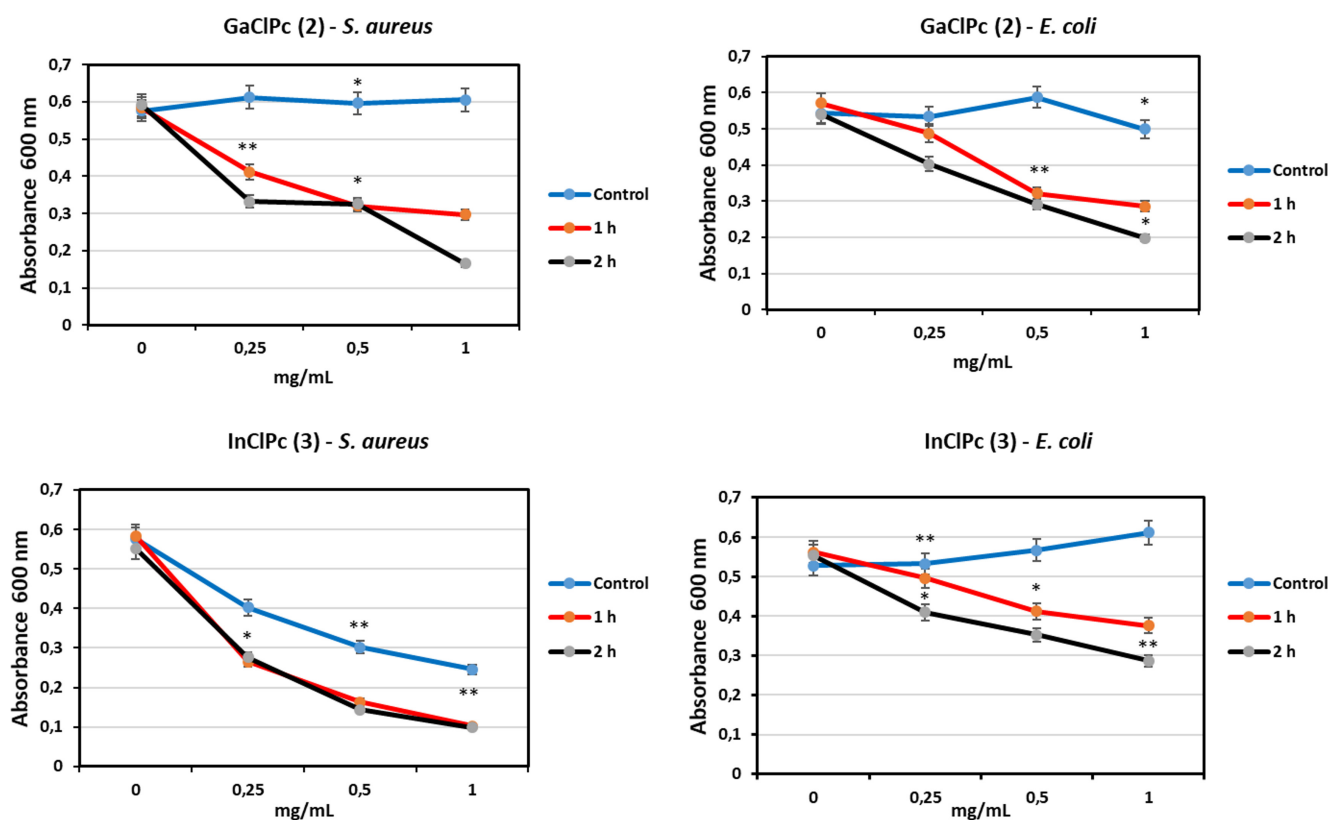
explained with the entrance of heavy metal ions into the microorganism cells and the formation of secondary metabolites which have heavy metals toxic for the microorganism. Heavy metal stress in the metabolic pathway of the organism results in the inhibition of bacterial growth (50).

Photodynamic antibacterial therapy. The antimicrobial effect of photoinactivation of Pcs was investigated toward *S. aureus* and *E. coli* as gram-positive and negative representative bacteria, respectively. Among all tested Pc compounds, GaClPc (2) and InClPc (3) demonstrated significant antimicrobial effects for tested microorganisms at 2 h of light irradiated samples (Fig. 3). Compound 2 showed a 71.35% inhibition effect against *S. aureus* and 63.53% for *E. coli* at 2 h light-irradiating while compound 3 exhibited an 82.98% inhibition effect against *S. aureus*. In other Pcs, the inhibition effect remained below 30%. With GaClPc (2) and InClPc (3), increasing the inhibitor concentration and light exposure increased the inhibition effect against tested microorganisms. In the control experiment performed without light-irradiation, only in the InClPc (3), inhibition was observed with increasing inhibitor concentration in parallel with the results obtained in the disk diffusion experiment. The inhibitory activity with light irradiation of compound 2 and compound 3 can be explained by the existence of -Cl substituents on the structure (51). In a study in which the antimicrobial activities of eutectic gallium–indium alloys for *E. coli* and *S. aureus* were explored, the viable counts of bacterial cells decreased sharply (52).

Photodynamic antimicrobial therapy was applied to the Pc compounds in many studies, and the effect of substituents and metal ions in the center of the Pc compounds was investigated. The most powerful photosensitizers were found as amphiphilic sulfonated zinc Pc and cationic tetramethylenepyridinium chloride of hydroxyaluminum phthalocyanine compounds for *E. coli* and *S. aureus* (42). When aluminum disulfonated phthalocyanine (AlPcS₂) was used as a photodynamic antibacterial agent against methicillin-resistant *S. aureus* (MRSA), low concentrations of AlPcS₂ after light irradiation could kill the MRSA (53).

Table 1. Antibacterial activity of InClPc (3) at 1 mg mL⁻¹ concentration and standard antibiotics against the tested bacteria.

Bacteria	ATCC 6051 <i>B. subtilis</i>	ATCC 25922 <i>E. coli</i>	ATCC 14579 <i>B. cereus</i>	ATCC 25923 <i>S. aureus</i>
InClPc (3)	8 ± 0.12 mm	-	11 ± 1.04 mm	8 ± 0.36 mm
Ampicillin (10µg disk ⁻¹)	-	-	-	23 ± 0.04 mm
Cefotaxime (30µg disk ⁻¹)	24 ± 0.09 mm	18 ± 1.02 mm	22 ± 1.06 mm	-


**Figure 3.** Photodynamic antimicrobial activities of GaClPc (2) and InClPc (3) for tested bacteria. (**P* < 0.05, ***P* < 0.001).

Antioxidant activity

DPPH free radical scavenging activity. When the scavenging abilities of the Pcs were examined, CoPc (4) presented the highest antioxidant potential at all tested concentrations (Fig. 4). Compound 4 showed even higher antioxidant activity than standard compound Trolox at 2000 µg mL⁻¹ concentration. The radical scavenging potential of Pc molecules reduced in the order of 4 > 6 > 5 > 7 > 3 > 2. The resonance of localized electrons has a direct effect on the antioxidant feature of Pcs, and π electron density is affected by central metal ion, electrovalent character and connected substituent. Besides, the redox capability of a metal ion increases the antioxidant activity (54).

In the study in which 4-(3,4,5-trimethoxybenzyloxy) phthalonitrile derivative phthalocyanine molecules were prepared and antioxidant features were studied by using DPPH assay, CoPc showed the highest antioxidant activity followed by nickel and zinc derivatives (55). In many studies examining the antioxidant potentials of substituted Pcs, the highest antioxidant activity was observed with CoPc which is in line with our study (54,56).

Reducing power. The results of the reducing power assay were given in Fig. 5. The reducing power indirectly indicates the total reducing potential of the studied compound and the color resulting from Fe³⁺ → Fe²⁺ reduction obtained by monitoring the

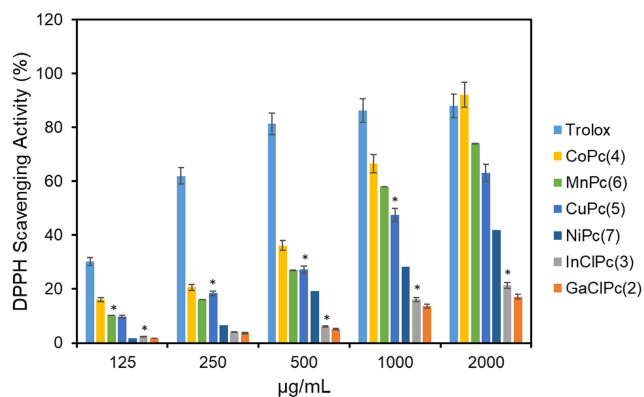


Figure 4. DPPH free radical scavenging activities of tested Pcs at different concentrations and standard compound Trolox. Values are expressed as the mean \pm SEM of three independent experiment. * $P < 0.05$.

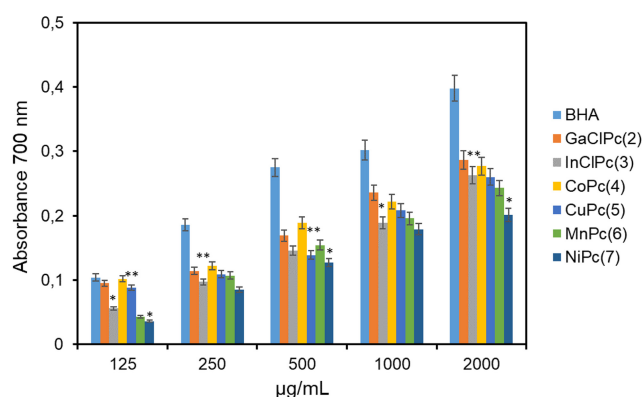


Figure 5. Reducing the ability of Pc compounds and standard compound BHA. Values are expressed as the mean \pm SEM of three independent experiment. * $P < 0.05$, ** $P < 0.001$.

change at 700 nm (43), and increasing absorbance value represented the increasing reducing effect.

Standard compound BHA demonstrated the maximum reducing activity at all tested concentrations. GaClPc (2) and CoPc (4) revealed the highest and similar reducing activity at all concentrations studied, followed by CuPc (5) > MnPc (6) > InClPc (3) > NiPc (7).

Determination of cytotoxic effects. According to MTT results, six compounds administered at doses of 50, 5 and 0.5 $\mu\text{g mL}^{-1}$ were found to have no significant cytotoxic effects on HEK-293, PANC-1, MDA-MB-231, HepG2, A549, HeLa and CaCo-2 cells.

Table 2. IC_{50} values of NO production and cytotoxic activities of compounds in LPS-activated RAW 264.7 cells.

Compounds	iNOS IC_{50} ($\mu\text{g mL}^{-1}$)	MTT IC_{50} ($\mu\text{g mL}^{-1}$)	iNOS IC_{50} (μM)	MTT IC_{50} (μM)
GaClPc (2)	12 \pm 5	ND	9 \pm 5	ND
InClPc (3)	7 \pm 0.5	ND	5 \pm 0.5	ND
CoPc (4)	27 \pm 8	ND	21 \pm 8	ND
CuPc (5)	6 \pm 1	36 \pm 2	5 \pm 1	28 \pm 2
MnPc (6)	34 \pm 3	>50	27 \pm 3	>40
NiPc (7)	41 \pm 2	>50	32 \pm 2	>40
Doxorubicin	5 \pm 0.01	>20	9 \pm 0.01	>34

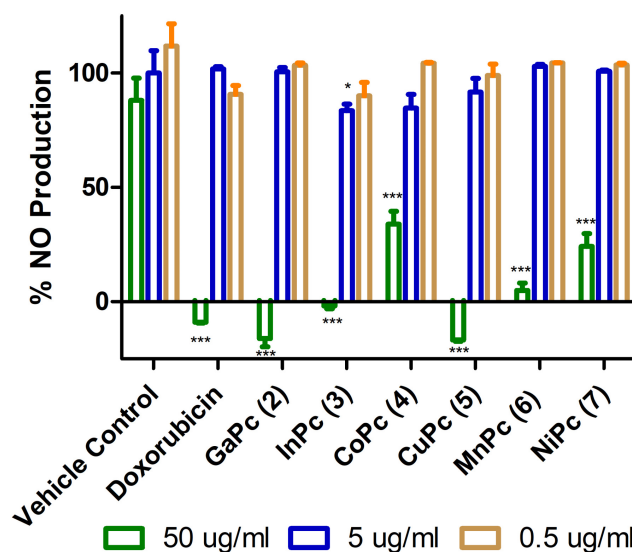


Figure 6. Inhibitory effects of tested compounds on LPS-induced nitrite formation by RAW 264.7 macrophages. Doxorubicin was used as 34, 3, 0.3 μM . * $P < 0.05$, *** $P < 0.001$ versus vehicle control cells.

Positive control doxorubicin IC_{50} values were found to be on cancer cells 5 \pm 0.4, 8 \pm 1, 21 \pm 2, 3 \pm 0.04, 24 \pm 1.5, 5 \pm 0.04 and 19 \pm 1 μM , respectively (Table S1, Figure S1), similar to other studies (57–59). Although the effect of doxorubicin was observed, the IC_{50} value could not be reached on macrophage cells (Table 2, Fig. 7). Relatively higher IC_{50} values could be seen in the literature (60). Moreover, the previous study reported that LPS prevents RAW 264.7 cells from doxorubicin-induced cell death (61). In addition, high cell concentrations are used for the iNOS assay; in the present study, the cytotoxicity tests of RAW 264.7 cells were performed following the iNOS assay. It has been reported that the cytotoxic activity of doxorubicin progressively decreases depending on the cell density (62). Low dark cytotoxicity of Pcs has been reported before due to the

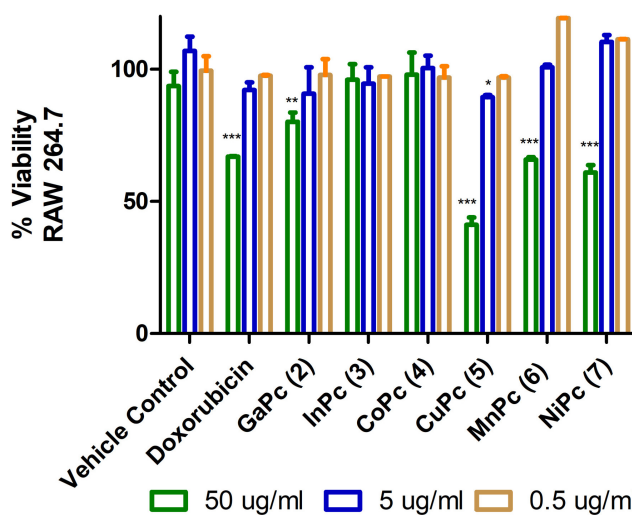


Figure 7. Effects of different concentrations of compounds on RAW 264.7 cells viability determined by the MTT assay. Doxorubicin was used as 34, 3, 0.3 μM . * $P < 0.05$, ** $P < 0.01$, *** $P < 0.001$ versus vehicle control cells.

absence of reactive oxygen species, and the results from the present study are in agreement with other studies (33,63,64). Therefore, their phototoxic effects should be studied to evaluate their anticancer potential.

iNOS assay. In murine macrophage RAW264.7 cells, LPS alone induces the transcription and protein synthesis of iNOS and raised nitric oxide (NO) formation. It is known that iNOS-mediated inhibition of NO production, which is known to be effective in many pathophysiological conditions, can display a role in anti-inflammatory and immunoregulatory activities (65). This cell-based assay system has been carried out for drug screening and the estimation of potential inhibitors of the pathways leading to the induction of iNOS and NO formation. According to the findings obtained, the percentage of NO production of samples applied at doses of 50, 5 and 0.5 $\mu\text{g mL}^{-1}$ in LPS-activated RAW264.7 cells was given in Fig. 6.

The results indicated that GaClPc (2), InClPc (3), CoPc (4), CuPc (5), MnPc (6) and NiPc (7) considerably inhibited NO production in LPS-activated RAW264.7 cells with IC_{50} values of 12 ± 5 , 7 ± 0.5 , 27 ± 8 , 6 ± 1 , 34 ± 3 and $41 \pm 2 \mu\text{g mL}^{-1}$, respectively, without exhibiting significant cytotoxic effects. Only in CuPc (5), the MTT IC_{50} value was reached as $36 \pm 2 \mu\text{g mL}^{-1}$ on RAW 264.7 cells. (Table 2, Fig. 7). The cytotoxic effect may be due to aggregation during the incubation which may disrupt the cell physiology.

These compounds have been shown the immunoregulatory effects (32,66). The lowest IC_{50} value was obtained in CuPc (5). It has been reported that copper complexes may have an anti-inflammatory effect in the literature (67). In addition to the treatment of inflammatory diseases, some tumor cells prefer the inflammatory environment (68). Therefore, Pcs that have got anti-inflammatory effects may be important therapeutic candidates for the treatment of various tumors.

CONCLUSION

Herewith, a series of water-soluble phthalocyanine compounds appended with sulfonated groups at non-periphery was prepared and evaluated. Antimicrobial activities were explored by using photodynamic antimicrobial inactivation technique, and light activation was applied to the synthesized Pcs at different times and inhibitor concentrations. Increased exposure to light and increased concentration elevated the antimicrobial activity with GaClPc (2) and InClPc (3). Compound 2 exhibited the maximum reducing power capacity among the studied compounds, and CoPc (4) showed even better free radical scavenging capacity than standard compound Trolox at $2000 \mu\text{g mL}^{-1}$ concentration. Among the compounds investigated within the scope of the study, phthalocyanines with central atoms gallium and indium have the potential to be used in the treatment of local infections in photodynamic inactivation studies. As a result of cytotoxicity studies of the phthalocyanine molecules toward cancer cell lines used in this study, it was observed that they have low dark cytotoxic effects. Further studies are required to phototoxic effects and anticancer potentials should be examined. However, the synthesized Pcs had significant inhibition of NO production especially GaClPc (2), InClPc (3) and CuPc (5) in LPS-induced macrophages. They may play an immunoregulatory role as a novel therapeutic alternative that deserves further detailed study.

Acknowledgment—The study was not supported by any organization.

CONFLICT OF INTEREST

There are no conflicts of interest reported by the authors.

DATA AVAILABILITY STATEMENT

The authors confirm that the data supporting the findings of this study are available within the article.

SUPPORTING INFORMATION

Additional supporting information may be found online in the Supporting Information section at the end of the article:

Table S1. Cytotoxic activity of the compounds on HEK-293, PANC-1, MDA-MB-231, HepG2, A549, HeLa and Caco-2 cells, IC_{50} values given as μM .

Figure S1. Cytotoxic effect of seven compounds on HEK-293 (A), PANC-1 (B), MDA-MB-231 (C), HepG2 (D), A549 (E), HeLa (F) and Caco-2 (G) cells after 48 h exposure to different sample concentrations. Cell viability was determined by MTT assay. Doxorubicin was used as positive control (H). Control was exposed to vehicle only which was taken as 100% viability. Data are expressed as mean \pm SD

Figure S2. MALDI-TOF Mass spectrum of 5.

Figure S3. MALDI-TOF Mass spectrum of 6.

Figure S4. MALDI-TOF Mass spectrum of 7.

Figure S5. FT-IR spectrum of 5.

Figure S6. FT-IR spectrum of 6.

Figure S7. FT-IR spectrum of 7.

Figure S8. UV-Vis absorption spectra of 2-7 in water (concentration $\sim 1 \times 10^{-6} \text{ mol dm}^{-3}$).

REFERENCES

- Basova, T. V., R. G. Parkhomenko, M. Polyakov, A. G. Gürek, D. Atilla, F. Yuksel, E. I. Ryabchikova, B. Y. Kadem and A. K. Hassan (2016) Effect of dispersion of gold nanoparticles on the properties and alignment of liquid crystalline copper phthalocyanine films. *Dye. Pigment* **125**, 266–273.
- Güzel, E. (2019) Dual-purpose zinc and silicon complexes of 1,2,3-triazole group substituted phthalocyanine photosensitizers: synthesis and evaluation of photophysical, singlet oxygen generation, electrochemical and photovoltaic properties. *RSC Adv.* **9**, 10854–10864.
- Jiang, Y., Y. Lu, X. Lv, D. Han, Q. Zhang, L. Niu and W. Chen (2013) Enhanced catalytic performance of Pt-free iron phthalocyanine by graphene support for efficient oxygen reduction reaction. *ACS Catal* **3**, 1263–1271.
- Basova, T. V., N. S. Mikhaleva, A. K. Hassan and V. G. Kiselev (2016) Thin films of fluorinated 3d-metal phthalocyanines as chemical sensors of ammonia: An optical spectroscopy study. *Sensors Actuators, B Chem.* **227**, 634–642.
- Koyun, O., S. Gorduk, M. Gencten and Y. Sahin (2019) A novel copper(II) phthalocyanine-modified multiwalled carbon nanotube-based electrode for sensitive electrochemical detection of bisphenol A. *New J. Chem.* **43**, 85–92.
- Lo, P.-C., M. Salomé Rodríguez-Morgade, R. K. Pandey, D. K. P. Ng, T. Torres and F. Dumoulin (2020) The unique features and promises of phthalocyanines as advanced photosensitizers for photodynamic therapy of cancer. *Chem. Soc. Rev.* **49**, 1041–1056.
- Almeida-Marrero, V., E. van de Winckel, E. Anaya-Plaza, T. Torres and A. de la Escosura (2018) Porphyrinoid biohybrid materials as an

- emerging toolbox for biomedical light management. *Chem. Soc. Rev.* **47**, 7369–7400.
8. Li, X., B. De Zheng, X. H. Peng, S. Z. Li, J. W. Ying, Y. Zhao, J. D. Huang and J. Yoon (2019) Phthalocyanines as medicinal photosensitizers: Developments in the last five years. *Coord. Chem. Rev.* **379**, 147–160.
 9. Zhang, Y. and J. F. Lovell (2017) Recent applications of phthalocyanines and naphthalocyanines for imaging and therapy. *Wiley Interdiscip. Rev. Nanomedicine Nanobiotechnology* **9**, e1420.
 10. Li, X., S. Lee and J. Yoon (2018) Supramolecular photosensitizers rejuvenate photodynamic therapy. *Chem. Soc. Rev.* **47**, 1174–1188.
 11. Al-Raqa, S. Y., K. Khezami, E. N. Kaya, A. Kocak and M. Durmuş (2021) Experimental and theoretical investigation of water-soluble silicon(IV) phthalocyanine and its interaction with bovine serum albumin. *J. Biol. Inorg. Chem.* **1**, 3.
 12. Chitgupi, U. and J. F. Lovell (2018) Naphthalocyanines as contrast agents for photoacoustic and multimodal imaging. *Biomed. Eng. Lett.* **82**(8), 215–221.
 13. Lovell, J. F. and P.-C. Lo (2012) Porphyrins and Phthalocyanines for Theranostics. *Theranostics* **2**, 815.
 14. Dumoulin, F., M. Durmuş, V. Ahsen and T. Nyokong (2010) Synthetic pathways to water-soluble phthalocyanines and close analogs. *Coord. Chem. Rev.* **254**, 2792–2847.
 15. Sobotta, L., J. Długaszewska, P. Kasprzycki, S. Lijewski, A. Teubert, J. Mielcarek, M. Gdaniec, T. Goslinski, P. Fita and E. Tykarska (2018) In vitro photodynamic activity of lipid vesicles with zinc phthalocyanine derivative against *Enterococcus faecalis*. *J. Photochem. Photobiol. B Biol.* **183**, 111–118.
 16. Revuelta-Maza, M. Á., E. Heras, M. Agut, S. Nonell, T. Torres and G. Torre (2021) Self-assembled binaphthyl-bridged amphiphilic AABB phthalocyanines: nanostructures for efficient antimicrobial photodynamic therapy. *Chem. – A Eur. J.* **27**, 4955–4963.
 17. Ghani, F., J. Kristen and H. Riegler (2012) Solubility properties of unsubstituted metal phthalocyanines in different types of solvents. *J. Chem. Eng. Data* **57**, 439–449.
 18. Gürel, E., M. Pişkin, S. Altun, Z. Odabaş and M. Durmuş (2015) Synthesis, characterization and investigation of the photophysical and photochemical properties of highly soluble novel metal-free, zinc(ii), and indium(iii) phthalocyanines substituted with 2,3,6-trimethylphenoxy moieties. *Dalt. Trans* **44**, 6202–6211.
 19. Lee, W., S. B. Yuk, J. Choi, D. H. Jung, S. H. Choi, J. Park and J. P. Kim (2012) Synthesis and characterization of solubility enhanced metal-free phthalocyanines for liquid crystal display black matrix of low dielectric constant. *Dye. Pigment* **92**, 942–948.
 20. Güzel, E., A. Koca, A. Gül and M. B. Koçak (2015) Microwave-assisted synthesis, electrochemistry and spectroelectrochemistry of amphiphilic phthalocyanines. *Synth. Met.* **199**, 372–380.
 21. van de Winckel, E., R. J. Schneider, A. de la Escosura and T. Torres (2015) Multifunctional logic in a photosensitizer with triple-mode fluorescent and photodynamic activity. *Chem. – A Eur. J.* **21**, 18551–18556.
 22. Bandera, Y., M. K. Burdette, J. A. Shetzline, R. Jenkins, S. E. Creager and S. H. Foulger (2016) Synthesis of water soluble axially disubstituted silicon (IV) phthalocyanines with alkyne & azide functionality. *Dye. Pigment* **125**, 72–79.
 23. Zhang, Y., Y.-K. Cheung, D. K. P. Ng and W.-P. Fong (2020) Immunogenic necroptosis in the anti-tumor photodynamic action of BAM-SiPc, a silicon(IV) phthalocyanine-based photosensitizer. *Cancer Immunol. Immunother.* **702**(70), 485–495.
 24. Çakir, D., V. Çakir, Z. Biyikliolu, M. Durmuş, H. Kantekin, D. Çakir, V. Çakir, Z. Biyikliolu, M. Durmuş, H. Kantekin, D. Çakir, V. Çakir, Z. Biyikliolu, M. Durmuş and H. Kantekin (2013) New water soluble cationic zinc phthalocyanines as potential for photodynamic therapy of cancer. *J. Organomet. Chem.* **745–746**, 423–431.
 25. Kuznetsova, N. A., N. S. Gretsova, V. M. Derkacheva, O. L. Kaliya and E. A. Lukyanets (2003) Sulfonated phthalocyanines: aggregation and singlet oxygen quantum yield in aqueous solutions. *J. Porphy. Phthalocyanines.* **07**, 147–154.
 26. Hanakova, A., K. Bogdanova, K. Tomankova, K. Pizova, J. Malohlava, S. Binder, R. Bajgar, K. Langova, M. Kolar, J. Mosinger and H. Kolarova (2014) The application of antimicrobial photodynamic therapy on *S. aureus* and *E. coli* using porphyrin photosensitizers bound to cyclodextrin. *Microbiol. Res.* **169**, 163–170.
 27. Dai, T., Y. Y. Huang and M. R. Hamblin (2009) Photodynamic therapy for localized infections-State of the art. *Photodiagnosis Photodyn. Ther.* **6**, 170–188.
 28. Hamblin, M. R. and T. Hasan (2004) Photodynamic therapy: A new antimicrobial approach to infectious disease? *Photochem. Photobiol. Sci.* **3**, 436–450.
 29. Cassidy, C. M., M. M. Tunney, P. A. McCarron and R. F. Donnelly (2009) Drug delivery strategies for photodynamic antimicrobial chemotherapy: From Benchtop to clinical practice. *J. Photochem. Photobiol. B Biol.* **95**, 71–80.
 30. Amaral, G. P., G. O. Puntel, C. L. Dalla Corte, F. Dobrachinski, R. P. Barcelos, L. L. Bastos, D. S. Avila, J. B. T. Rocha, E. O. Da Silva, R. L. Puntel and F. A. A. Soares (2012) The antioxidant properties of different phthalocyanines. *Toxicol. Vitro.* **26**, 125–132.
 31. Abdel-Maksoud, M. S., M. I. El-Gamal, M. M. Gamal El-Din, Y. Choi, J. Choi, J. S. Shin, S. Y. Kang, K. H. Yoo, K. T. Lee, D. Baek and C. H. Oh (2018) Synthesis of new triarylpyrazole derivatives possessing terminal sulfonamide moiety and their inhibitory effects on PGE2 and nitric oxide productions in lipopolysaccharide-induced RAW 264.7 macrophages. *Molecules* **23**, 2556.
 32. Ayaz, F., A. Yuzeer and M. Ince (2018) Immunostimulatory effect of Zinc Phthalocyanine derivatives on macrophages based on the pro-inflammatory TNF α and IL1 β cytokine production levels. *Toxicol. Vitro.* **53**, 172–177.
 33. Yalazan, H., B. Barut, B. Ertem, C. Ö. Yalçın, Y. Ünver, A. Özel, İ. Ömeroğlu, M. Durmuş and H. Kantekin (2020) DNA interaction and anticancer properties of new peripheral phthalocyanines carrying tosylated 4-morpholinoaniline units. *Polyhedron* **177**, 114319.
 34. Senapathy, G. J., B. P. George and H. Abrahamse (2020) Enhancement of phthalocyanine mediated photodynamic therapy by catechin on lung cancer cells. *Molecules* **25**, 4874.
 35. Miller, J. W. (2008) Higher irradiance and photodynamic therapy for age-related macular degeneration (An AOS thesis). *Trans. Am. Ophthalmol. Soc.* **106**, 357–382.
 36. Chan, W. S., N. Brasseur, C. La Madeleine, R. Quellet and J. E. Van Lier (1997) Efficacy and mechanism of aluminium phthalocyanine and its sulphonated derivatives mediated photodynamic therapy on murine tumours. *Eur. J. Cancer* **33**, 1855–1859.
 37. Tempête, C., C. Giannotti and G. H. Werner (1992) Identical photosensitizing activities of a sulfonated aluminium phthalocyanine on human erythroleukemia cell lines susceptible or resistant to the cytotoxic activity of doxorubicin. *J. Photochem. Photobiol. B Biol.* **14**, 201–205.
 38. Lee, E. N., H. J. Cho, C. H. Lee, D. Lee, K. C. Chung and S. R. Paik (2004) Phthalocyanine tetrasulfonates affect the amyloid formation and cytotoxicity of α -synuclein. *Biochemistry* **43**, 3704–3715.
 39. Güzel, E., A. Koca and M. B. Koçak (2017) Anionic water-soluble sulfonated phthalocyanines: Microwave-assisted synthesis, aggregation behaviours, electrochemical and in-situ spectroelectrochemical characterisation. *Supramol. Chem.* **29**, 536–546.
 40. Güzel, E., G. Yaşa Atmaca, A. Erdoğan and M. B. Koçak (2017) Novel sulfonated hydrophilic indium(III) and gallium(III) phthalocyanine photosensitizers: preparation and investigation of photophysical and photochemical properties. *J. Coord. Chem.* **70**, 2659–2670.
 41. Biemer, J. J. (1973) Antimicrobial susceptibility testing by the Kirby-Bauer disc diffusion method. *Ann. Clin. Lab. Sci.* **3**, 135–140.
 42. Ryskova, L., V. Buchta, M. Karaskova, J. Rakusan, J. Cerny and R. Slezak (2012) In vitro antimicrobial activity of light-activated phthalocyanines. *Cent. Eur. J. Biol.* **8**, 168–177.
 43. Sağlam, Ö., M. Akin, H. Pekbelgin Karaoğlu, N. Saki and M. B. Koçak (2020) Investigation of time-kill evaluation and antioxidant activities of new tetra-substituted metallophthalocyanines bearing 4-(Trifluoromethoxy)thiophenyl groups. *ChemistrySelect* **5**, 2522–2527.
 44. Güzel, E., N. Şaki, M. Akin, M. Nebioğlu, İ. Şişman, A. Erdoğan and M. B. Koçak (2018) Zinc and chloroindium complexes of furan-2-ylmethoxy substituted phthalocyanines: Preparation and investigation of aggregation, singlet oxygen generation, antioxidant and antimicrobial properties. *Synth. Met.* **245**, 127–134.
 45. Mosmann, T. (1983) Rapid colorimetric assay for cellular growth and survival: Application to proliferation and cytotoxicity assays. *J. Immunol. Methods* **65**, 55–63.
 46. Crisafulli, C., M. Galuppo and S. Cuzzocrea (2009) Effects of genetic and pharmacological inhibition of TNF- α in the regulation of inflammation in macrophages. *Pharmacol. Res.* **60**, 332–340.

47. Güzel, E., Ü. M. Koçyiğit, P. Taslimi, S. Erkan and O. S. Taskin (2021) Biologically active phthalocyanine metal complexes: Preparation, evaluation of α -glycosidase and anticholinesterase enzyme inhibition activities, and molecular docking studies. *J. Biochem. Mol. Toxicol.* **35**, 1–9.
48. Mikula, P., L. Kalhotka, D. Jancula, S. Zezulka, R. Korinkova, J. Cerny, B. Marsalek and P. Toman (2014) Evaluation of antibacterial properties of novel phthalocyanines against *Escherichia coli* - Comparison of analytical methods. *J. Photochem. Photobiol. B Biol.* **138**, 230–239.
49. Çelik, Ç., N. Farajzadeh, M. Akin, G. Y. Atmaca, Ö. Sağlam, N. Şaki, A. Erdoğan and M. B. Koçak (2021) Investigation of the biological and photophysical properties of new non-peripheral fluorinated phthalocyanines. *Dalt. Trans.* **50**, 2736–2745.
50. Chudobova, D., S. Dostalova, B. Ruttkay-Nedecky, R. Guran, M. A. M. Rodrigo, K. Tmejova, S. Krizkova, O. Zitka, V. Adam and R. Kizek (2015) The effect of metal ions on *Staphylococcus aureus* revealed by biochemical and mass spectrometric analyses. *Microbiol. Res* **170**, 147–156.
51. Saki, N., M. Akin, A. Atsay, H. R. Pekbelgin Karaoglu and M. B. Kocak (2018) Synthesis and characterization of novel quaternized 2, 3-(diethylmethylamino)phenoxy tetrasubstituted Indium and Gallium phthalocyanines and comparison of their antimicrobial and antioxidant properties with different phthalocyanines. *Inorg. Chem. Commun.* **95**, 122–129.
52. Li, L., H. Chang, N. Yong, M. Li, Y. Hou and W. Rao (2021) Superior antibacterial activity of gallium based liquid metals due to Ga³⁺-induced intracellular ROS generation. *J. Mater. Chem. B* **9**, 85–93.
53. Griffiths, M. A., B. W. Wren and M. Wilson (1997) Killing of methicillin-resistant *Staphylococcus aureus* in vitro using aluminium disulphonated phthalocyanine, a light-activated antimicrobial agent. *J. Antimicrob. Chemother* **40**, 873–876.
54. Snow, A. W. (2003) Phthalocyanine aggregation. In *The Porphyrin Handbook: Phthalocyanines: Properties and Materials*, pp. 129–176. Academic Press, Amsterdam.
55. Salih A rtaş, M., B. Cabir and S. Özdemir (2013) Novel metal (II) phthalocyanines with 3,4,5-trimethoxybenzyloxy- substituents: Synthesis, characterization, aggregation behaviour and antioxidant activity. *Dye. Pigment* **96**, 152–157.
56. Bilgicli, A. T., Y. Tekin, E. H. Alici, M. N. Yaraşir, G. Arabaci and M. Kandaz (2015) α - or β functional phthalocyanines bearing thiophen-3-ylmethanol substituents: Synthesis, characterization, aggregation behavior and antioxidant activity. *J. Coord. Chem.* **68**, 4102–4116.
57. Sobolewska, D., A. Galanty, K. Grabowska, J. Makowska-Wąs, D. Wróbel-Biedrawa and I. Podolak (2020) Saponins as cytotoxic agents: An update (2010–2018). Part I-steroidal saponins. *Phytochem. Rev.* **19**, 139–189.
58. Tabanca, N., A. Nalbantsoy, P. E. Kendra, F. Demirci and B. Demirci (2020) Chemical characterization and biological activity of the mastic gum essential oils of *Pistacia lentiscus* var. chia from Turkey. *Molecules* **25**, 2136.
59. You, J., F. Gao, H. Tang, F. Peng, L. Jia, K. Huang, K. Chow, J. Zhao, H. Liu, Y. Lin and J. Chen (2019) A medicinal and edible formula YH0618 ameliorates the toxicity induced by Doxorubicin via regulating the expression of Bax/Bcl-2 and FOXO4. *J. Cancer* **10**, 3665–3677.
60. Ma, L., H. C. Bygd and K. M. Bratlie (2017) Improving selective targeting to macrophage subpopulations through modifying liposomes with arginine based materials. *Integr. Biol. (United Kingdom)* **9**, 58–67.
61. Hassan, F., S. Islam, M. M. Mu, H. Ito, N. Koide, I. Mori, T. Yoshida and T. Yokochi (2005) Lipopolysaccharide prevents doxorubicin-induced apoptosis in RAW 264.7 macrophage cells by inhibiting p53 activation. *Mol. Cancer Res.* **3**, 373–379.
62. Kobayashi, H., Y. Takemura and T. Ohnuma (1992) Relationship between tumor cell density and drug concentration and the cytotoxic effects of doxorubicin or vincristine: Mechanism of inoculum effects. *Cancer Chemother. Pharmacol.* **31**, 6–10.
63. Zhao, Y. Y., J. Y. Chen, J. Q. Hu, L. Zhang, A. L. Lin, R. Wang, B. Y. Zheng, M. R. Ke, X. Li and J. D. Huang (2021) The substituted zinc(II) phthalocyanines using “sulfur bridge” as the linkages. Synthesis, red-shifted spectroscopic properties and structure-inherent targeted photodynamic activities. *Dye. Pigment* **189**, 109270.
64. Shao, J., J. Xue, Y. Dai, H. Liu, N. Chen, L. Jia and J. Huang (2012) Inhibition of human hepatocellular carcinoma HepG2 by phthalocyanine photosensitizer Phthalocyanine: ROS production, apoptosis, cell cycle arrest. *Eur. J. Cancer* **48**, 2086–2096.
65. Yoon, W.-J., Y. M. Ham, K.-N. Kim, S.-Y. Park, N. H. Lee, C.-G. Hyun and W. J. Lee. (2009) Anti-inflammatory activity of brown alga *Dictyota dichotoma* in murine macrophage RAW 264.7 cells.
66. Yüzer, A., F. Ayaz and M. Ince (2019) Immunomodulatory activities of zinc(II)phthalocyanine on the mammalian macrophages through p38 pathway: Potential ex vivo immunomodulatory PDT reagents. *Bioorg. Chem* **92**, 103249.
67. Brown, D. H., W. E. Smith, J. W. Teape and A. J. Lewis (1980) Antiinflammatory effects of some copper complexes. *J. Med. Chem* **23**, 729–734.
68. Allen, S. G., Y.-C. Chen, J. M. Madden, C. L. Fournier, M. A. Altemus, A. B. Hiziroglu, Y.-H. Cheng, Z. F. Wu, L. Bao, J. A. Yates, E. Yoon and S. D. Merajver (2016) (2016) Macrophages enhance migration in inflammatory breast cancer cells via RhoC GTPase signaling. *Sci. Rep.* **61**(6), 1–11.